Journal of Modern Processes in Manufacturing and Production, Volume 9, No. 4, Autumn 2020

DOR: 20.1001.1.27170314.2020.9.4.6.4

Research Paper

Evaluation of Optimal Conditions, Microstructure, and Mechanical Properties of Aluminum to Copper Joints Welded by FSW

Ahmad Afsari[1*], Shahin Heidari[2], Jaleel Jafari[1]

[1]Department of Mechanical Engineering, Shiraz Branch, Islamic Azad University, Shiraz, Iran

[2]Bone and Joint Diseases Research Center, Shiraz University of Medical Sciences, Shiraz, Iran, P. O. Box: 71348-14336

[*]Email of Corresponding Author: afsari@iaushiraz.ac.ir

Received: September 16, 2020; Accepted: February 21, 2021

Abstract

The joining of dissimilar metals by Friction stir welding (FSW) is one of the newest metal joining processes. In this research, the tool was made from H13 hot working steel, which has a concave shoulder with a 3-degree inclined angle. The welding operation performed using a milling machine. The non-homogeneous workpieces joining of the Al alloy (5083) and a sheet of annealed copper (ASTM B36) with a thickness of 2 mm was investigated by the FSW method. The joining process was carried out at three tool transverse speeds of 25, 35, and 45 mm per minute and three rotational velocities of 1000, 1300, and 1600 rpm. Microstructural changes of the welded samples were analyzed by optical microscopy and scanning electron microscopy used to distinguish the type of phases. While its mechanical properties analyze according to different parameters used in the experiments. Also, the welded parts were subjected to microhardness and tensile tests. It found that the welding sample with a tool rotational speed of 1300 rpm and a forward speed of 35 mm/min has the best mechanical properties, with a tensile strength of 82% and a yield strength of 80% of aluminum base metal. While welded components with a forward speed of 25 mm/min have tunnel defects and brittle phases of AlCu and Al_2Cu formed in the stir region so that with the increase of rotational speed and forward speeds, the percentage of these brittle phases increases.

Keywords

Non-homogeneous Metals, Friction Stir Welding (FSW), Aluminum Series 5xxx, Copper Alloy ASTM B36, Mechanical Properties

1. Introduction

The Friction stir welding (FSW) process involves a non-consumable rotary tool consisting of a pin and shoulder, so it is necessary to move the tool to the adjacent edges of the two sheets and then move along the seam of the joint. The heat inside the workpiece is produced by the friction between the pin and the shoulder of the tool with the metal, causes severe plastic deformation of the job. In this method, the maximum heat produced should be 0.8 percent of the base metal. Local heating softens the material around the pin and, in combination with the tool rotational and linear motion, moves the metal from the front of the pin backward, thereby filling the back cavity, which is created by the tool moving forward.

On the other hand, by applying pressure to the metal, by the shoulder of the tool, which is located above the softened area, thereby creating a bond between the two parts. The front of the tool restricts the flow of metal to a level equal to the frontal position. As a result, the tool operates, and its impact on the workpiece results in a solid-state connection. The tool's three primary tasks are to warm up the workpiece, to move the material to create a bond, and also to keep the doughy metal under the tool forehead.

The essential FSW parameters are the welding process and machine parameters. The parameters of the welding process include the rotational tool speed, forward speed, tools off-center, the direction of rotation, tool angle, axial force, and workpiece restraint force. In contrast, the device parameters include shoulder diameter, shoulder geometry, pin geometry, pin penetration in a workpiece, pin diameter, and tool material. In this method, the angle between the pin and the workpiece is critical. An appropriate angle between the pin and the workpiece will cover the material moved by the shoulder as it crosses the welding border. It will prevent heat dissipation and avoid the softened material from escaping through the tool. So the pressure in the dough area will increase, and the connection will be better.

The diverse applications of non-homogenous joints in power plants, military purposes, and the electronics industry have resulted in non-homogenous metal welding using various fusion and solid-state methods. Freezing defects, the formation of intermetallic compounds, and excessive heat input in fusion welding processes have made these processes less attractive for bonding non-homogeneous metals. Despite the suitability of some solid-state joining methods such as ultrasonic welding, intrusive and explosive welding for non-homogeneous metal joining, some limitations of these processes such as geometrical constraints, required special equipment and high cost have led to extensive research on solid-state joining processes to remove these restrictions [1]. The amount of heat in the FSW process was determined by the forward speed, rotational speed, as well as the amount of heat dissipation per unit area. Increasing the rotational speed increases the input heat and decreasing the rotational speed, decreases the input heat to the workpiece. On the contrary, it has the opposite effect of speed. That is, increasing the forward speed reduces the heat and decreases the forward speed, increasing the inlet heat. On the other hand, the higher the heat dissipation, will be lower the boiling temperature.

High heat in FSW causes various defects in the weld. These defects are recognizable by the appearance of the weld. Examples include the small bubbles of the welding surface and the abrasion of the welding surface. At higher temperatures, dough material under the shoulder and extrusion of the metal occurs, which creates a crease and chip around the weld line. If the temperature is too high, the weld metal is very dilute and cannot withstand the applied force. It will damage the weld metal, welding tool, and piece backing plate in the automated processes that involve a constant load to the workpiece during the process.

Pure aluminum is a weak metal whose tensile strength varies between 90 and 150 MPa depending on the type of operation. For this reason, its use is limited to the production of electrical conductors and home appliances. Aluminum alloys have been developed for use in structural applications and, depending on the type and amount of alloying elements and kind of heat treatment applied, can have a strength of up to 500 MPa. These alloys are classified into two major categories: aluminum cast alloys and used aluminum alloys. Aluminum alloy 5083 has 4% magnesium and about 0.25%

chromium. This alloy is widely used in the production of aircraft oil and fuel pipes, fuel tanks, chemical equipment that requires excellent corrosion resistance, good fatigue strength, weldability, and moderate strength [3, 2]. Research has been carried out on the FSW of aluminum to copper and accomplished the appropriate bonding between the two metals, but the bonding often fails in mechanical tests from the nugget or contact surface of the two metals. There are several reasons to justify this, including the formation of brittle intermetallic compounds such as Al_4Cu_9 and Al_2Cu as well as the formation of a low-strength oxide layer of Al_2O_3 and CuO in the vicinity of intermetallic compounds [4].

Gritman et al. [5] have proposed a new method of FSW of aluminum, which increases the heat generated by increasing the rotational tool speed. Most of the heat generated in this method is provided by friction of the shoulder with the metal surface. On the other hand, the surface of the shoulder prevents contact with the surrounding area, heat dissipation, and oxidation of the base metal. A study by Mahoney et al. [7] entitled Properties of FSW 7075 T651 aluminum ", shows that the high temperature of this area affects the sediments and alloying elements. Sometimes the high temperature of the heat-affected area dissolves the sediment and expands the free area in the heat-affected zone. In a study conducted by Liu et al. [9], entitled "Weld appearance and microstructural characteristics of FSW butt barrier welded joints of aluminum alloy to copper", it was shown that in this case, different properties of base metal and weld metal could produce oscillatory stresses in heat affected areas and adjacent areas of the weld. These stresses cause welding fatigue, which will eventually lead to the development of cracks and damage to the joint. Since the different properties of the metal vary with temperature, it is difficult to predict the non-homogenous bonding behavior of the weld metal under mathematical calculations. In these conditions, only the experimental tests can indicate the lifetime of the joints.

Bhamji et al. [10] in a study entitled ", Linear FSW of aluminum to copper," were able to weld aluminum 1050 to Cu-101C using FSW. They have described the FSW process as a suitable method for joining non-homogeneous metals such that the bonds obtained exhibit excellent electrical and mechanical properties. Ismaili et al. [11] bonded aluminum to copper as well as aluminum and brass sheets by FSW, and by examining their mechanical and microstructural properties, they found that the highest strength obtained was 80% of the base metal strength of aluminum. They explained the reason for this proper joining because of the right flow of materials and the creation of narrow multi-layer intermetallic compounds in the joint as well as the production of a composite structure in the stir zone. They also reported that by diverging from the optimal welding parameter, the size of the particles in the stir zone increased, and the defects increased in this zone, leading to the transfer of the crack growth path from the boundary to the confluence region.

The research conducted in this article was aimed at obtaining experimental results to determine the physical and mechanical properties and microstructure analysis of the joint obtained by the FSW process for materials Aluminium - Copper. The welding operation performed using a milling machine. the non-homogeneous workpieces joining of the Al alloy (5083) and a sheet of annealed copper (ASTM B36) with a thickness of 2 mm was investigated by the FSW method. The main welding parameters applied were: rotating speed of the rotating element 1300 rev/min, speed of the rotating element 25 mm / min.

2. Materials and Methods

Initially, the workpiece raw materials were prepared and cut to the desired size for welding operations. Then the welding process was performed with different parameters, and finally, the welds were subjected to microstructural and mechanical tests, and the results were evaluated. The first step in this study was the preparation of cold-worked 5083 aluminum alloy sheets and annealed B36 copper with a thickness of 2 mm as joining materials. Then to determine the chemical composition, the prepared materials were subjected to quantitative analysis. The results of these analyzes are presented in Tables 1 and 2. Next, the sheets were cut to 15 x 5 cm to be ready for the welding operation.

Table 1. Chemical Composition of Aluminum Alloy (5083)

Alloy Elements of Aluminum	Al	Cu	Cr	Mn	Mg	Fe	Si
Percentage	96.72	0.03	0.15	0.07	2.55	0.23	0.25

Table 2: Chemical Composition of Copper Alloy (B36)

Alloy Elements of Copper	Al	Cu	Cr	Mn	Mg	Fe	Si
Percentage	96.72	0.03	0.15	0.07	2.55	0.23	0.25

In this research work, H13 tool steel uses to perform the welding process. For this purpose, steel rods of 14 mm diameter were first cut into 8 cm long pieces. In the next step, the said parts were cut to produce a welding tool with a concave shoulder at a 3^{o} inclination angle, while the tool had a cylindrical pin of 1.6 mm length and a diameter of 3 mm. To increase its hardness and working life it was subjected to heat treatment by carburization at 1020 ° C, so that, its hardness reached 52 Rockwell. The welding operation performed using an FP4M milling machine, and the welding process was performed at rotational speeds of 1000, 1300, and 1600 RPM and Transverse speeds of 25, 35, and 45 mm/min the parameters and conditions of the welding process given in Table 3.

Table 3. Welding Process Parameters and Conditions

Sample Number	**Rotational speed (RPM)**	**Transverse speed (mm/Min.)**	**Sample Number**	**Rotational speed (RPM)**	**Transverse speed (mm/Min.)**
1	1000	25	6	1300	45
2	1000	35	7	1600	25
3	1000	45	8	1600	35
4	1300	25	9	1600	45
5	1300	35			

The sheets were first paired together and fastened in such a way that during the welding operation, the copper plate was positioned at the advancing side, and the welding direction was perpendicular to the rolling direction of the aluminum alloy. Figure 1 shows the sheets enclosed in the clamp during welding.

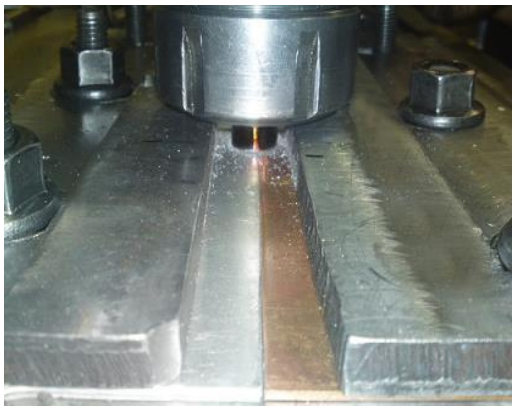

Figure 1. Set up of welding sheets and tool

Next, the seam of the joint and surrounding areas washed using acetone to eliminate possible contamination. After the washing operation, it was allowed enough time for the acetone to evaporate and completely dislodge the joint. The welding process carried out using an inclination angle of 2.5 degrees, a penetration depth of 0.4 mm and a rotating tool clockwise the 75% of the offset pin was in the aluminum base metal. Then the tool shoulder and pin were cleaned using a wire brush to maintain the tool's performance in the subsequent process. After preparing the samples, microstructural and mechanical tests were performed to determine the optimum welding parameters.

3. Microstructural examination

After the welding process, metallographic operations carried out to examine the microstructure of the samples in five stages: grinding, mounting, sanding, polishing, and etching. The cross-sectioning of the specimens was performed by a laboratory incision perpendicular to the welding line. While mounting operation, after thoroughly cleaning the specimens of any dirt, grease, and other additives and placing the components exactly in the center of the mounting mold, a cold mount, of two-part mix consisting of resin and hardener, was used, the use of cold type mounts to prevent the microstructure of the specimens being altered in this operation, and sanding operations were performed on 5 samples by soft sanding with grades of 400, 600, 800, 1200 and 2500 to polish the samples, special felt polish and diamond paste were used. The polishing process using diamond paste took between 20 and 30 minutes to remove all scrunch resulting from sanding, and the samples were etched, finally, the microstructural examination was performed by an optical microscope. For the etching of aluminum 5083, a modified Poulton's solution containing 12 mol of hydrochloric acid, 6 mol of nitric acid, 1 mol of fluoric acid, and 1 mol of water was used, while 40% ammonia in water used for the copper plate. The metallographic samples were etched in etch solution for a few moments and then washed and dried. The microstructural examination performed using an Olympus-type optical microscope (BH-2) with different magnifications. Then the microstructural features were analyzed using Image-j software.

3.1 Microhardness test

Vickers microhardness test performed by Shimadzu Micro-Harness Machine (TIP M). This test presented a hardness profile on the cross-section of the welded parts and in the center of the stir

zone using a weight of 100 g for 15 seconds. While the microhardness points are considered 100 μm apart.

3.2 Tensile test

For investigating the mechanical properties of the welded joints, the tensile test was performed by an Instron 5502 model 20-ton tensile machine with a speed of 1 mm/min. The specimens for tensile tests were prepared following ASTM E8 standard and perpendicular to the weld line so that the junction was placed in the center of the sample. In order to eliminate the stress concentration due to the decrease in the thickness created at the intersection due to the tool shoulder dip in the sheet, the surface of the tensile specimens was machined until all samples reached the same thickness. The dimensions of the sample stretch and the image of a real sample are shown in Figure 2.

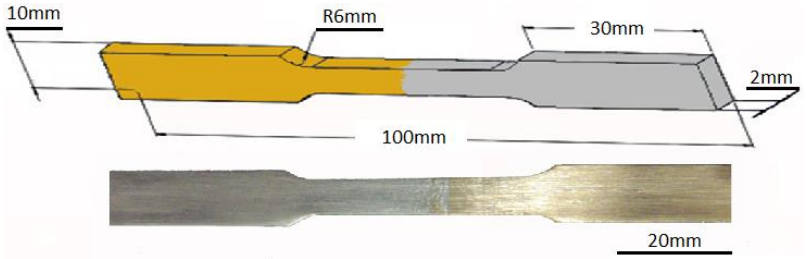

Figure 2. (A) Dimensions of the stretch sample and (B) The actual sample prepared

3.3 Scanning Electron Microscopy

Scanning electron microscopy of the model Leica Cambridge-S360 and energy dissociation method used to investigate the type of phase formed by the welding process. For this purpose, the prepared specimens were used for microstructural analysis by optical microscope.

4. Results and discussion

Figure 3 shows the basic microstructure of aluminum and copper alloys before welding. As shown in Figure 3(A), the initial aluminum alloy grains are elongated, which clearly the elongation shows the direction of rolling the sheet. In Figure 3(B) the initial grain size of the copper plate is shown to be co-axial and confirms that the prepared sheet annealed, while the initial grain size is about 40 μm.

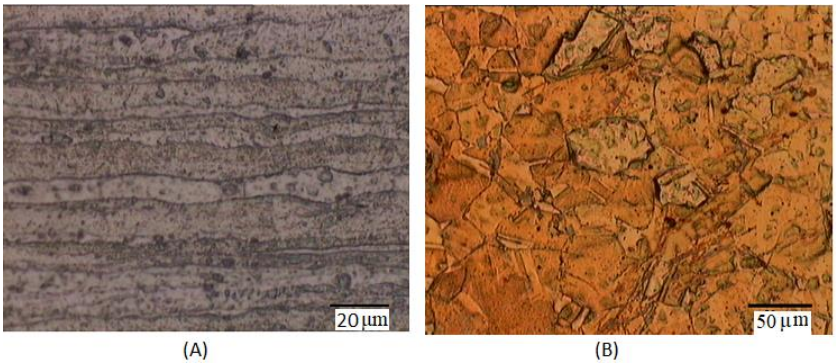

Figure 3. Base metal microstructure of (A) aluminum alloy (5083) and (B) copper alloy (B36)

Welding surface profiles of all samples are shown in Fig. 4. It can be seen that samples (a) and (c) have surface tunnels indicating a lack of proper connectivity in these samples. Non-proper bonding

and tunneling defects in these specimens may be due to the inadequate welding heat at a rotational speed of 1000 rpm, which is the lowest rotational speed in this study. Increasing the rotational speed of the tool increases the amount of heat generated by FSW. Rising temperatures lead to more paste metal and make the material flow easier due to the tool rotation, resulting in better continuity. On the other hand, increasing the rotational speed of the tool increases the strain and mixes more materials in the stir zone. In this regard, samples (a) and (c) due to low inlet temperature have insufficient flow materials, and the stirring has not performed well, which may be the reason for the lack of proper continuity in these samples. The size of the surface tunnel in sample number (c) is larger than sample number (a). Since the forward speed in samples (c) and (a) is 45 and 25 mm/min, respectively, so due to the higher forward speed of sample (c), the heat produced in this sample will be lower than that of sample (a). This lower heat makes the flow of the sample more difficult to obtain and the quality of the weld is lower.

The images show that by increasing the rotational speed from 1000 to 1,300 rpm, the surface of the specimens has smoothed and the defects removed. The increase in heat due to the rotational speed of the tool results in better material flow and allows the cause of obviation of defects in this rotational speed. But the specimen (f) welded at a speed of 1300 rpm and a forward speed of 45 mm/min have a rough surface than specimens 4 and 5, and some parts of the surface exhibit a disadvantage of welding surface wear. This may be due to the higher forward speed of this sample than the other two welded samples at a rotational speed of 1300 rpm due to the reduced heat produced, resulting in a lower material flow in the sample, which also results in welding surface wear. Excessive rotational speed increases the temperature and consequently increases the fluidity of the material. The high fluidity of the material increases the rate of material extrusion from the tool shoulder as well as the pleats due to the pressure applied to the base metal by the tool shoulder. This increase in extrusion results in a decrease in the surface area of the weld, which may lead to a decrease in the properties and quality of the weld. As can be seen in Figure 4, samples (g), (h), and (i), which have a maximum rotational speed of 1600 rpm, had more pleats than the other specimens, so the cause a lot of pleats is due to the high rotational speed and increased heat input. Besides, the pleats rate in sample (i) is lower than the other two welded samples at a rotational speed of 1600 rpm, ie samples (g) and (h). Higher forward speed in this specimen than in the other two specimens reduces input heat, fluidity, and also less material extrusion under the tool shoulder.

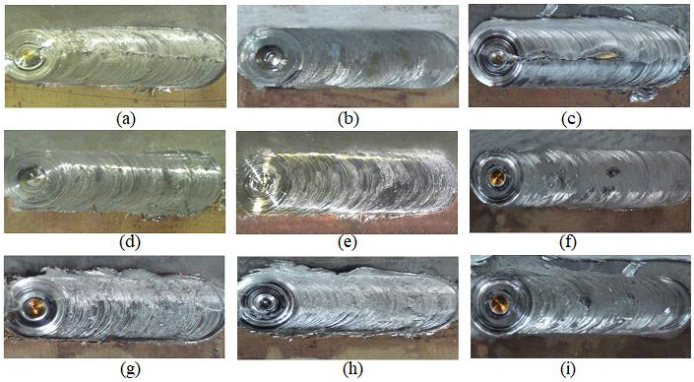

Figure 4. Surface profile of welded specimens

According to Figure 4(g), it is seen that the sample number (g) has a long crack at the beginning of its welding and it is expected that the sample does not have suitable properties. Excessive extrusion of materials in this sample may be the cause of this defect. Material extrusion reduces the volume of material underneath the tool shoulder, resulting in insufficient force from the tool to the weld metal and as a result, the forging operation behind the tool shoulder is not performed well. Inadequate forging of material underneath the tool shoulder can lead to poor bonding and longitudinal cracking. Samples (b), (e), and (h) are sound and no defects are observed on the surface of these welds. Since all of these specimens were welded at a forward speed of 35 mm/min. The forward speed of 35 mm/min appeared to be suitable for achieving smooth contiguity in this study, while at other forward speeds, defective specimens were found.

4.1 Welding Macrostructure

Metallographic samples from the cross-section of the welds prepared, and after sanding and etching operations, the quality of the welds, the amount and type of defects investigated. The macroscopic image of the welded specimens with a rotational speed of 1000 rpm shown in Figure 5.

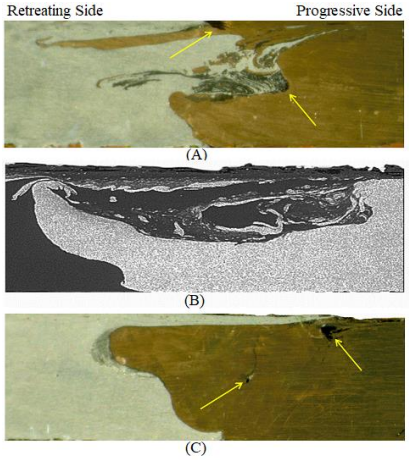

Figure 5. Macrostructure of welded samples

The low input heat in the FSW is the cause of the lack of proper mixing of the two pieces of material and therefore complete adaptation does not occur at the connection joint. Also, if the inlet temperature is low, fine harder metal particles are to disperse in the softer field. On the other hand, as the inlet heat rises, the material flow increases, and the particle size of the harder material diffuses into the more malleable base metal can grow more, and this has been confirmed in another research [11].

According to Figure 5, it observed that the material mixing speed is better at the forward momentum of 25 mm/min and the higher mixing rate in this sample is due to the higher heat input due to the lower forward speed. This higher heat makes the material flow better than other materials, and the mixing is also better. By increasing the forward momentum to 35 mm/min, as shown in Figure 5(B), the blending decreased, while at 45 mm/min due to the low heat input, the material flow was deficient, and the mixing was anomalous. The inappropriate mixture of this sample is due to the low heat in this sample since the join is not well performed in this sample, the mechanical properties of the join expected to be less satisfactory.

In sample (a) there is a tunnel fault at the surface and depth of the sample. The presence of a tunnel at the sample surface due to the appearance of the weld surface and the surface groove shown in Figure 5(A), it is expected that the high heat of welding due to the low forward speed in this specimen will increase the fluidity of the metal, leading to a decrease in the thickness of the metal due to excessive extrusion of the metal from the tool. Reducing the volume of material underneath the tool reduces the amount of pressure applied to the metal and the forging action by the tool shoulder does not perform well and increases the likelihood of tunneling defects and hence causes broken weld. Therefore, the low forward speed of this sample can attribute to the tunneling defects. There is also a tunnel defect in the surface and depth of the sample (c). The high speed of advancement of the tool may be the cause of these flaws. The high speed of welding causes the production heat to decrease, resulting in lower material flow and poor material flow. On the other hand, the senior forward momentum causes the material not to have enough time to move from the front to the back of the pin and fill the cavity behind it, creating the tunnel in the sample. Unlike the forward speed of 25 and 45 mm/min, the specimen produced at a forward rate of 35 mm/min is thorough, which is expected to have excellent mechanical properties.

The macroscopic image of the welded specimens at a rotational speed of 1300 rpm illustrated in Figure 6. Sample (d) has a small tunnel in the center of the weld. As mentioned earlier, the high temperature of welding can be the cause of this defect. Figure 6(B) shows the welded sample at a forward speed of 35 mm/min. There is no defect in this sample, and the welding is quite sound. The narrow bulb rings in this sample represent the proper flow of materials and create a uniform composite structure at the center of the sample. Figure 6(C) shows the macrostructure of sample (f). It can seem that there is no flaw in this sample, but the flow of materials is insufficient, and the mixing is not performed well. The lower heat in this sample than in the other two samples due to the higher forward speed of flow has led to lower material flow and inadequate mixing.

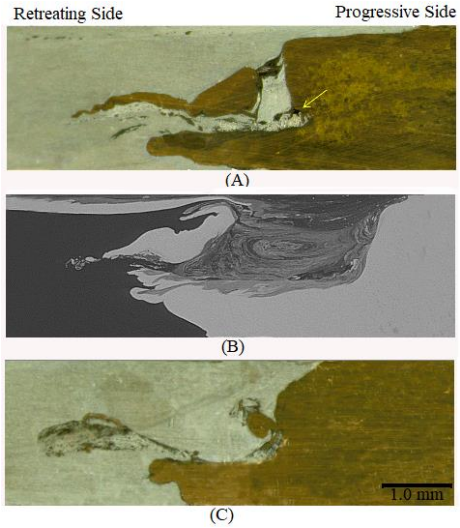

Figure 6. Welding macrostructure of samples (d), (e), and (f)

Figure 7 shows the welding macrostructure of the welded specimens at a rotational speed of 1600 rpm. As shown in Figure 7(A), mixing of materials is sufficient at a forward rate of 25 m/Min. so the copper and aluminum are well mixed. Still, large tunnels are seen in the center of the stir region

as well as at the copper and aluminum boundary on the regression of the weld, which can be due to the high heat of welding. It should be noted that sample (g) has the most top rotational speed and the lowest forward speed among all samples because it experiences the highest heat input among all samples

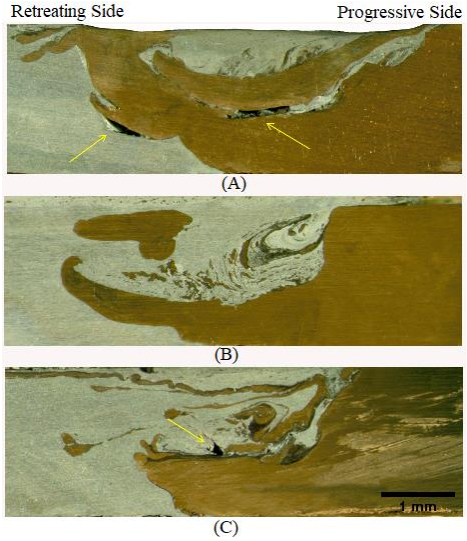

Figure 7. Structure of welding of samples (g), (h), and (a)

In Figure 5 (B)**,** the mixing is well done, and the size of the dispersed copper particles in the aluminum field is smaller than the sample in Figure 7(C). Also, the sample was utterly flawless and no defects were found in it. Sample (i) has reasonably good mixing, but a tunnel flaw was observed in the sample center. The reason for this flaw is the high forward speed because it does not allow the material to move to the back of the tool and fill the back cavity.

Based on the macroscopic images presented, it can be seen that the welded specimens are sound at a forward speed of 35 mm/min at all rotational speeds. Still, at other speeds, however, defective specimens have been observed. Therefore, it can be concluded that the forward speed of 35 mm/min is more suitable for thorough welding than the speeds of 25 and 45 mm/min. Also, all-welded specimens have tunneling defects at a speed of 25 mm/min. This indicates that the speed of 25 mm/min is too low for this type of welding, and this may cause the specimens to become defective. Therefore, the higher the heat generated at this speed and the lot of dislodgment of metal will result.

4.2 Welding Microstructure

Since the corrosion behavior of the two alloys in the etchant is very different, so it is, therefore, difficult to study the microstructure of all the samples and is virtually impossible. In this regard, sample (e) was selected for investigation and subjected to etching. Sample (e), which appeared to be flawless and in which proper mixing occurred in the welding stir zone, was typically studied to investigate the microstructure of the weld metal and its surrounding areas. Figure 8 shows the microstructure of the base metal and the heat-affected zone of the copper alloy. The grain size in the heat-affected region is larger than the base phase. Larger grains in this zone are due to heat applied during welding, which causes grain growth.

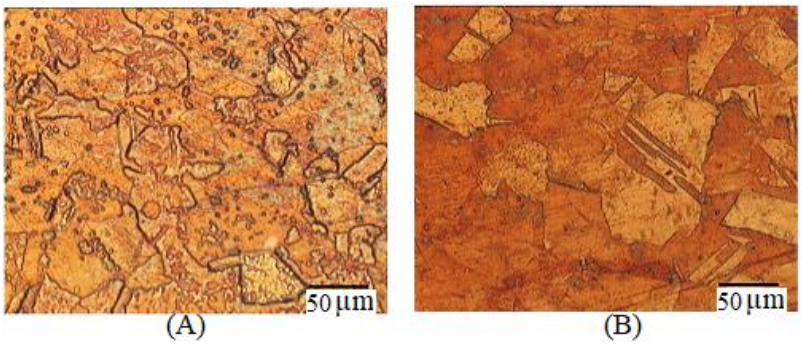

Figure 8. Copper alloy microstructure, (A) base metal, and (B) heat-affected zone

Figure 9(A) shows the microstructure of the base metal and Figure 9(B) the microstructure of the heat-affected zone, In the first, the grains are elongated along the direction of rolling and the later one, grain growth is aimed at removing the primary orientation structure and becoming the co-axial structure.

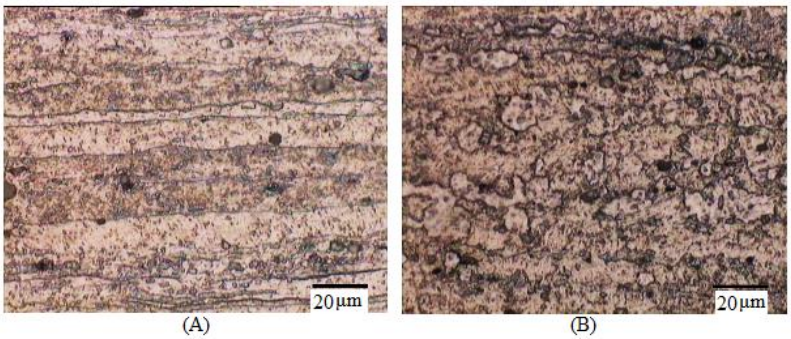

Figure 9. Aluminum alloy microstructure (A) base metal and (B) heat-affected zone

Since in FSW, there is low input heat and short heating time and on the other hand aluminum alloy in this research is located on the retreating side of the weld which experiences less heat than the progressive side, so the grain growth in the heat-affected zone is not high. As can be seen in Fig. 9, grain growth does not wholly eliminate the orientation structure, and the orientation structure due to cold-temperature operation is still observed in the heat-affected region. Also, in some areas, where directional grains were removed, grain growth was not high, and fine grains formed in this area. Therefore, in this case, it is expected that the hardness of the heat-affected region on the retreating side will not be much lower than that of the base metal. Figure 10 shows the microstructure of the region affected by the thermomechanical welding operations on the progressive side. Grain elongation in this situation is due to thermomechanical actions in the zone. The width of the area affected by thermomechanical activities in this sample is approximately 80 µ m. Since the heat in the retreating side is lower than the forward side, so the area affected by the thermomechanical operation on the backside is not much different from the heat-affected zone [12]. Figure 11 shows the aluminum microstructure in the stir weld region.

Figure 10. Zone of thermomechanical operations of copper (progressive side)

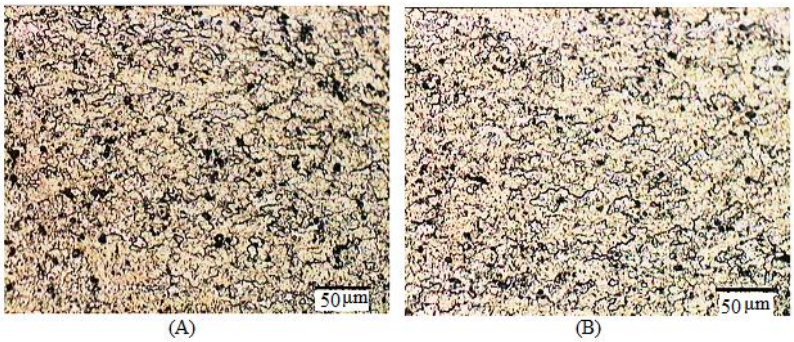

Figure 11. Microstructure of the stir zone (A) center of welded and (B) zone near the welded surface

The microstructure of this region is wholly recrystallized, fine-grained, and co-axial. The reason for this elegant structure is the continuous dynamic recrystallization and breakage of the primary grains due to the rotational motion of the tool. By measuring the grains size in the stir region, this sample shows that the average grain size above the stirred area and close to the weld surface is about 6 µ m, whereas in the center of the weld, have an average size of 5 µ m. Since in the FSW process, most of the heat input comes from the friction between the surface of the shoulder and the base metal, the near-surface areas in this process experience the most heat during welding. By moving away from the weld surface and moving deeper into the stir zone, the temperature decreases. This decrease in temperature from the surface to the bottom of the sample causes the grain growth to be higher than the depth after the dynamic recrystallization at the weld surface. Therefore, grains in areas near the surface of the weld are usually larger than areas farther from the surface as can be seen in Figure 11.

4.3 Micro Hardness

The graph of the hardness changes with distance from the welding center shown in Figure 12. In this figure, the hardness variations for the two welded specimens at rotational speeds of 1000 and 1300 rpm and with a forward rate of 35 mm/min compared. As can be seen at the rotational speed of 1000 and 1300 revolutions per minute, the hardness of the stir zone is higher than the hardness of both base metals. Three different dynamical recrystallization factors, composite formation in the stir zone, and intermetallic compounds due to the reaction between the non-homogeneous base metals can be attributed to the high hardness in this region. The dynamic recrystallization occurring in the stir region is due to the high dynamic recrystallization energy of copper alloys because, in the frictional welding process, these alloys do not recrystallize. In contrast, this phenomenon occurs in aluminum alloys. Dynamic recrystallization causes the structure of the stir region to be fine-grained

and co-axial. These finer grains cause the hardness of the stir region to be higher than that of the base metal in the FSW process.

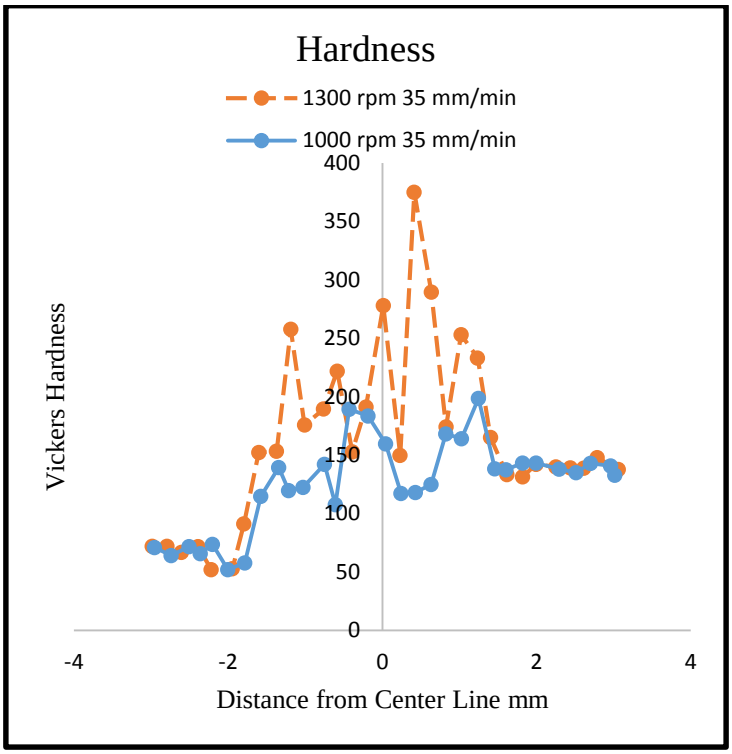

Figure 12. Diagram of welding hardness changes with distance from the welding center and with increasing rotational speed

The second factor that can increase the hardness in the agitation zone is the formation of a composite in the stir zone. The harder fine particles distributed in, the softer field will cause the harder the uniformity. The structure of the perturbation zone is fine-grained, and these finer and coherent grains cause the hardness of the agitation zone in the FSW process to be higher than the hardness of the base metal. The third cause of intermetallic compounds is due to the reaction between non-homogeneous base metals such that this reaction is formed at high welding temperatures and as a result of local melting of the base metal in this region because they require activation energy to form these compounds which are provided by heat. It seems that the combination of these three factors has increased the hardness in the stir region of this sample and besides, the amount of hardness in the stir region of this sample is highly fluctuating. The reason for this significant fluctuation can be attributed to the uneven distribution of copper alloy particles in aluminum and the formation of more intermetallic compounds near these particles. In other words, in areas where there are more mixing of aluminum and copper, more and more uniform intermetallic compounds can be formed, which increases the hardness in the region.

The heat-affected zone of this specimen on the retrograde side that is on the aluminum metal side is detectable by a hard drop in this region. As shown in Figure 11, in the area affected heat of aluminum, grain growth occurred due to the application of heat. This grain growth eliminated the elongated grains produced in the base metal during the cold working process, so for this purpose hardness was reduced in this sample. On the advancing side, the severe change of hardness in the

heat-affected area is not noticeable. Since the copper alloy used in this study was annealed, so the grain size in the area affected heat in the progressive direction will not change much. It will be the reason for the low change in this area.

In the welded sample with a rotational speed of 1300 rpm, the hardness number is higher, and the hardness fluctuation rate is lower. The higher the input heat in this process, the higher the grain growth after recrystallization, resulting in larger recrystallized grains. At a rotational speed of 1300 rpm, the input heat is higher than the speed of 1000 rpm, which will cause more grain growth in this sample. On the other hand, increasing the rotational speed will increase the strain in the stir region, resulting in smaller recrystallized grains [11, 1]. Also, as the rotational speed increases, the inlet heat increases, resulting in a higher stir temperature. This increase in temperature increases the probability of the formation of an intermetallic compound in the sample. As the amount of intermetallic compounds increases, so does the hardness, which has been proven by other researchers [13].

At both rotational speeds, the hardness on the forward side of the weld is higher than on the retreating side. Because FSW produces more heat on the forward side than on the backward side, it is more likely that intermetallic compounds will be more on this side. It could also be the reason for the higher hardness on the forward side of these samples. The peak of intermetallic compounds has been exacerbated by increasing rotational speeds and thus increasing input heat. This indicates that at more than 1,300 revolutions per minute, more intermetallic compounds are produced than at 1000 revolutions per minute, this is why hardness is higher in this sample. The combination of these factors increases the hardness at a speed of 1300 rpm compared to a speed of 1000 rpm.

4.4 Tensile test results

Tensile strength values of the welded specimens with different rotational speeds and forward speeds are shown in Figure 13. Sample (e) welded at a speed of 1300 rpm, and a forward speed of 35 mm/min has the highest tensile strength among all specimens. The tensile strength of this sample is 189 MPa, which is 82% of the tensile strength of the base metal aluminum. According to samples b and d, Figure 13 is entirely flawless, and mixing in the stir region is well performed. So the high strength in this sample seems natural. According to this graph, it can show that at all rotational speeds, the most upper tensile strength was observed for the welded specimens at a forward speed of 35 mm/min. This indicates that this forward speed is the optimum speed for welding.

At a forward speed of 35 mm/min by increasing the rotational speed from 1000 to 1600 rpm, as shown in Figure 13, the tensile strength first increased and then decreased, so that the maximum tensile strength at 1300 rpm have obtained. Considering the samples c, d and e, in Figure 13, it shows that sample (b), that is a sample welded at a rotational speed of 1000 rpm despite the absence of defects in the stir zone, and surrounding areas, the mixing of materials is not in the range of sample (e). The lower mixture in this sample may be due to the lower strength in this sample. On the other hand, by increasing the rotational speed of the tool to 1600 rpm, the inlet heat is increased, and the intermetallic compounds are more likely to form. Intermetallic compounds will reduce the strength and flexibility of the weld. Therefore, the reason for the decrease in the strength of the sample (h) can be attributed to the formation of intermetallic compounds due to the increased rotational speed [14].

At a forward speed of 25 mm/min, as shown in the macroscopic images, there are tunneling defects at all three speeds in the stir zone. This defect causes the specimens to break early, and as a result, as shown in Figure 13, the strength decreases sharply.

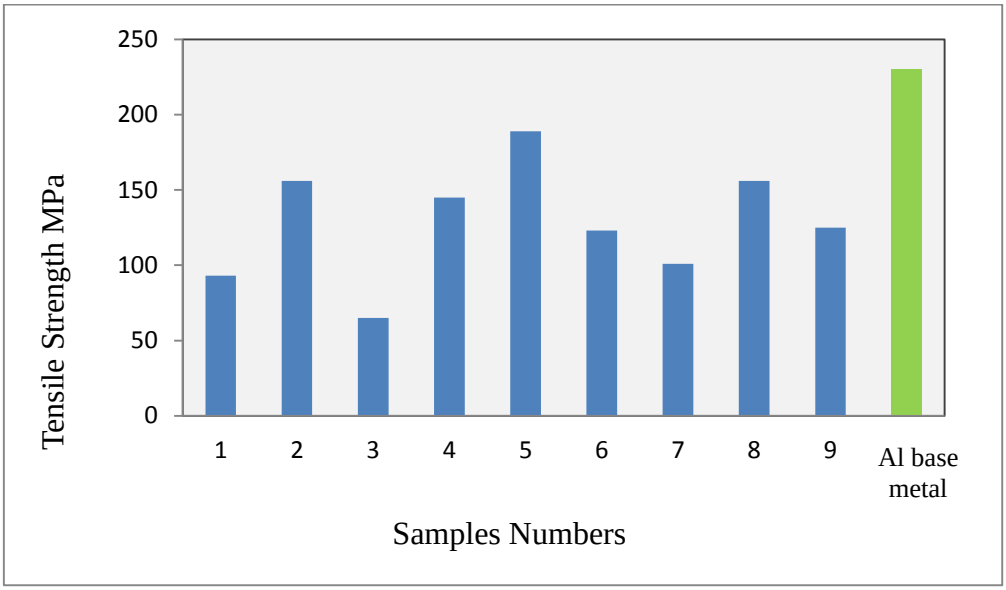

Figure 13. Tensile strength of welded specimens

Sample (c), produced with the lowest rotational speed and maximum forward speed used in this study, has the lowest input heat among all samples. As shown in Figure 4(c) in the macroscopic image of this sample, there is a large surface tunnel in the center of the sample. The same large tunnel significantly reduced the strength, and therefore this sample has the lowest strength. The amount of defects in the weld has a significant effect on the yield strength of the welded specimens. Also, according to the Hall – Patch relation, the yield strength is inversely correlated with the size of the recrystallized grain, meaning that the smaller the grain size, the higher the yield strength. Another critical factor affecting yield strength is the brittle constituents between the metal formed in the stir zone and the boundary of the weld that reduce the yield strength. The yield strength of the welded specimens in Figure 14 compared with each other. It is quite evident that the highest yield strength was related to sample (e) which is 80 % of the tensile strength of the aluminum base metal.

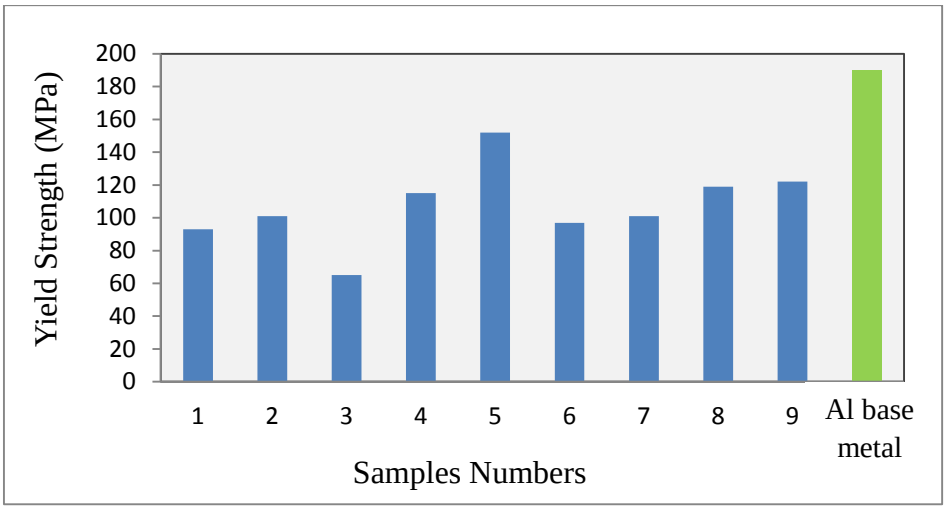

Figure 14. The yield strength of the welded specimens

As can be seen, the welded specimens with a forward speed of 35 mm/min are entirely flawless. They have higher yield strength than the specimens produced with the same rotational speed, indicating that this forward speed is suitable for bonding. In all three samples provided at this forward speed, failure occurred in the stir region. In sample (b), the mixing of materials is not as large as samples (e) and (h). The same may be the reason for the lower yield strength of this sample compared to the sample (e). On the other hand, in the sample (h), which has experienced more inlet heat than the previous two samples, increased intermetallic brittle compounds and the presence of larger coarser grains than the sample (e) may be the reasons for the lower yield strength of this sample.

According to Figure 15, it can be seen that the percentage of elongation of all samples is lower than that of aluminum base metal (5083). The defects, in addition to the brittle intermetallic compounds formed in the stir zone and the aluminum and copper boundaries, are due to a decrease in the percent elongation of these samples [14].

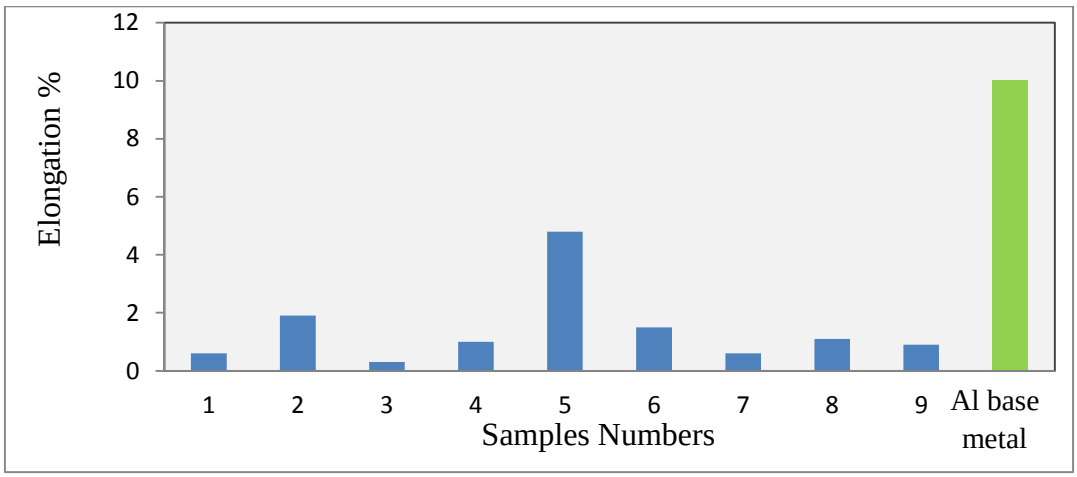

Figure 15. Percentage of elongation of welded specimens

The welded specimens at 35 mm/min had a higher elongation than the specimens produced at similar rotational speeds, in which the among them the highest percentage of elongation is related to

sample (e) which also had the highest yield strength and tensile strength. The lowest rate of elongation also corresponds to the sample (c), which had the lowest heat during welding. Inadequate heat in this sample has caused tunneling defects and poor mixing in this sample, which may be the reason for its early failure and low elongation. As shown in Figures 13 and 14, this sample did have the lowest tensile strength and yield strength.

4.5 X-ray diffraction analysis

The formation of brittle intermetallic phases is one of the problems of non-homogeneous welding, the formation of these brittle phases causes brittle bonding, welding brittle metal as a result of the formation of these phases with thermal stresses caused by thermal mismatches, resulting in the formation of transverse micro-cracks in the weld metal, which ultimately destroys the bonding properties. On the other hand, due to the remarkable role of non-homogenous joints in reducing raw material prices and improving design conditions, the demand for these fittings is increasing. In FSW, if the welding parameters are not well adjusted, excessive heat is transferred to the welding components, and this causes the intermetallic phases to form locally. Due to the higher heat applied to the progressive side of the weld, the amount of these compounds in the progressive side will be higher than the retreating side. Thus the formation of these phases results in a decrease in the mechanical properties of the joint and increases the hardness of the stir region, which is consistent with the results of other researchers [12]. The formation of these phases in non-homogeneous friction welded joints indicates a high rotational speed relative to the forward speed. According to relation 1, the heat input due to welding has a direct and inverse relationship with the square of the rotational speed and the forward speed. Therefore, the heat input of the weld, resulting in the formation of brittle intermetallic compounds, is strongly dependent on the rotational speed, showing a decrease in tensile strength and a reduction in the percentage of increase in elongation, which is consistent with the results of other researchers [3].

$$\frac{T}{T_m} = k\left(\frac{\omega^2}{V}\right)^{\alpha} \quad (1)$$

In this respect, T- metal temperature, Tm- melting temperature, ω- rotational speed, V- forward speed, and K and α are constant-coefficient with values of $0.04 < \alpha < 0.06$ and $0.65 < k < 0.75$.

In the present study, X-ray analysis was performed to investigate the formation of these phases in weld metal from fracture surface of specimens welded at 35 mm/min and three rotational speeds of 1000, 1300, and 1600 rpm. The results of this analysis given in Figure 16 as a comparison. As can be seen, due to the presence of one or two peaks of AlCu and Al_2Cu phases, there is a possibility of the formation of AlCu and Al_2Cu intermittent brittle phases in the weld metal of this sample. As the rotational speed to forward speed increases, the peak intensities associated with these brittle phases also increased. According to Equation 1, increasing the ratio of rotational speed to forwarding speed, increases the temperature and increases the temperature resulting in local melting and formation of these phases. Therefore, the creation of inter-metal brittle phases due to the welding heat increases the hardness of the weld metal and this increase will lead to a decrease in flexibility and ultimately a reduction in the mechanical properties of the weld. In this regard, the increase in hardness mentioned is a confirmation of the formation of intermittent brittle phases due to the rise

in input heat, and the latter is due to the increase in rotational speed, which was observed in the X-ray analysis in figure 16. Figure 17 illustrates the hardness of the two points in the stir region of samples (b) and (e) for comparison.

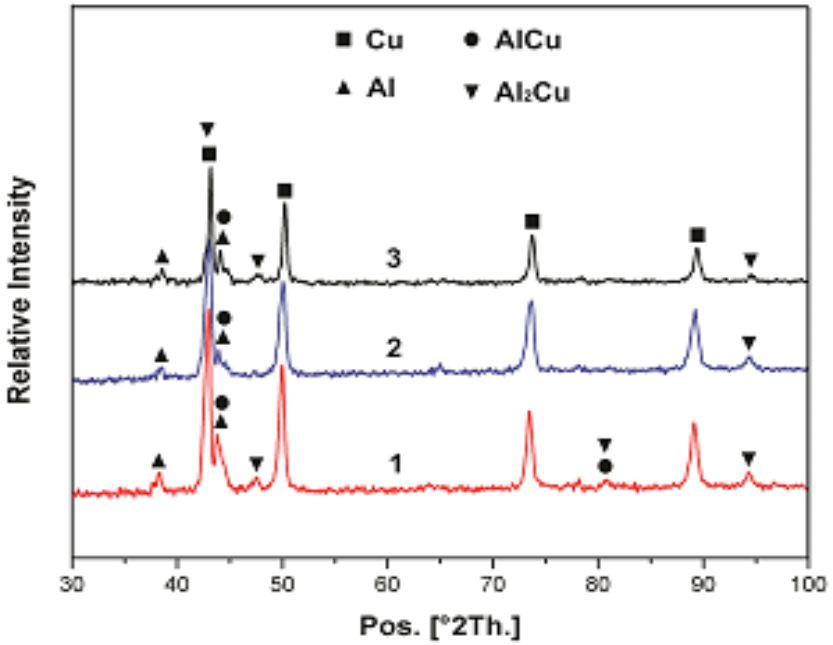

Figure 16. X-ray analysis on the fracture surface of tensile test specimens for sample (h), (2) (e), (3) (b)

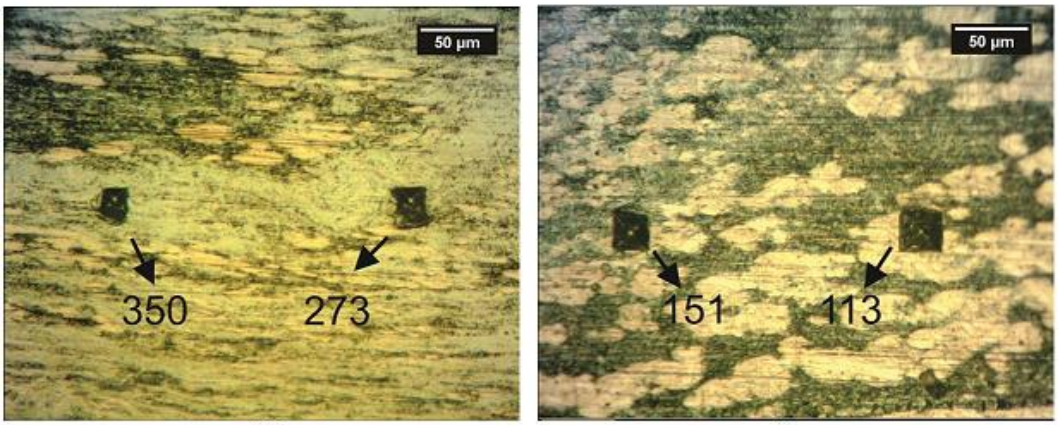

Figure 17. The effect of the formation of brittle intermetallic phases on the hardness of the Nagget zone, (A)-sample (e) and (B) Sample (b) (harnesses based on Vickers)

As can be seen, the hardness in the sample nugget zone (e) is higher than the hardness in the sample nugget zone (b). The EDS analysis obtained from sample nugget (e) shown in figure 18 also confirms the results of the X-ray analysis.

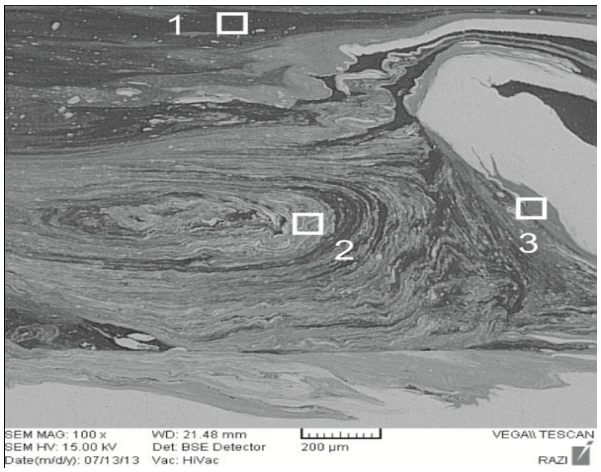

S.NO.:	Cu	Al	Zn	Mg
1	0.90	96.21	0.16	2.72
2	40.43	55.78	1.17	2.62
3	27.82	68.91	5.61	1.66

Figure 18. EDS analysis prepared from sample nugget section (e)

4.6 EDS Analysis

EDS analysis was performed on a map and point basis, respectively, to investigate the chemical composition as well as the distribution of different elements from the sample cross-sections. Sample map analysis (b) is shown in Figure 18. Also, sample EDS analysis (e) is shown in Figure 19.

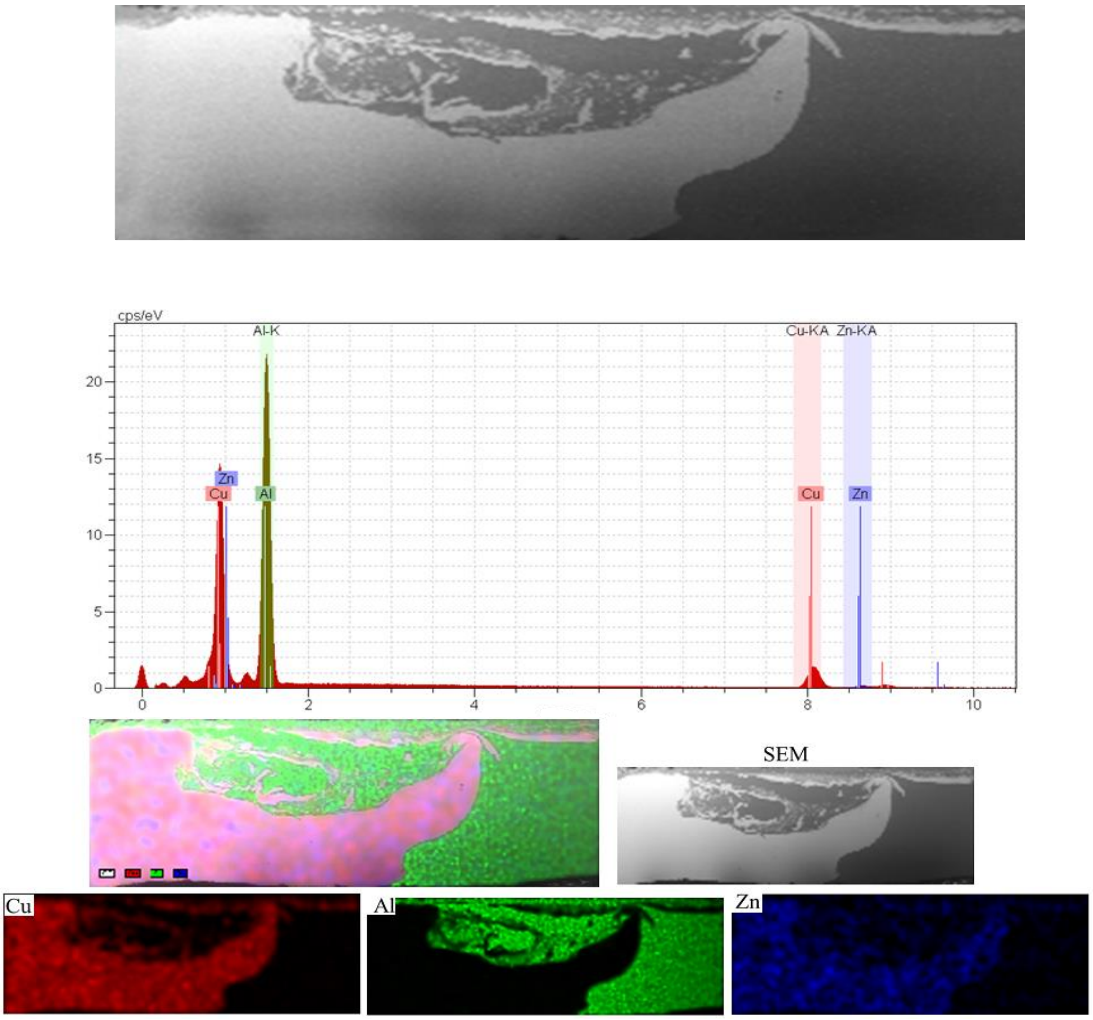

Figure 19. Map analysis of how different elements are distributed in the weld metal

As can be seen in the SEM image of the sample area of sample (e), based on the light intensity of the Nougat region's image can be subdivided into the dark, grey, bulbous, and bright areas. In the SEM image taken with the back-electron mode, the change in light intensity means the difference in chemical composition. As a result, a point is drawn from these EDS analysis areas, and the results are shown in Figure 20.

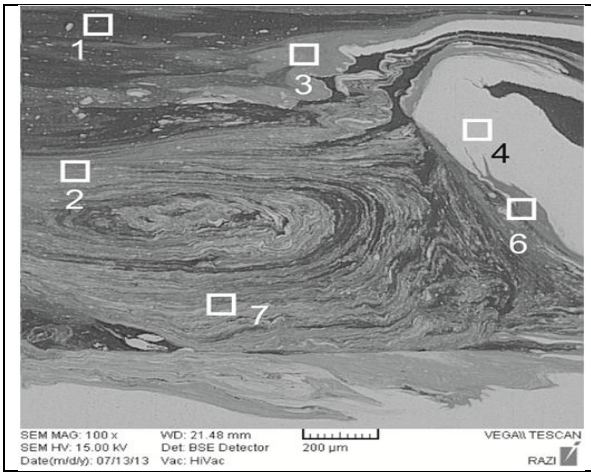

S.NO.:	Cu	Al	Zn	Mg
1	2.10	95.14	0.34	2.43
2	42.28	54.83	1.27	1.42
3	23.82	70.95	3.41	1.82
4	91.67	---	8.33	---
5	27.82	68.91	5.61	1.66
6	5.33	45.78	1.47	2.32

Figure 20. Spot analysis of welding cross-section (atomic percent) of sample (e)

5. Conclusions

In this study, non-homogeneous Aluminum (5083) sheets cold worked and copper (B36) annealed sheets were bonded by the FSW method. The optimum welding parameters, the joining process performed at three different, forward speeds and rotational speeds, and the properties and microstructure of the welds analyzed. The results are as follows.

-The parameters related to the sample (e) with a rotational speed of 1300 rpm and a forward speed of 35 mm/min, have the best mechanical properties so that the tensile strength of this sample is 82% and its yield strength is 80% of the base aluminum. As a result, the optimal welding parameters in this research are considered.

-All welded specimens with a forward speed of 35 mm/min have the least defects and have desired mechanical properties. While all-welded samples with a forward speed of 25 mm/min due to low temperatures, the material does not ferment well and it is hard to weld. This increases the density of the misplacements, resulting in reduced material flow, leading to defects such as lack of surface filling or tunnel defects.

-The probability of the formation of AlCu and Al_2Cu brittle phases in the stirred region increased so that the percentage of these phases increased as the rotational speed ratio forward speed increased. In this respect, constant forward speed, if rotational speed increases, leads to a higher hardness in the stirred region, which could be due to the higher percentage of brittle intermetallic compounds at a higher rotational speed.

-The presence of brittle intermetallic compounds has resulted in a decrease in the strength and the percentage of elongation of the specimens. While the percentage of elongation of all samples decreased significantly compared to the base metals, so the defects such as surface

incompleteness or tunnel defects, as well as existing geometric defects, in addition to the intermittent brittle compounds formed, can be the reason for this.

6. References

[1] Esmaeili, A., Givi, M.B. and Rajani, H.Z. 2011. A metallurgical and mechanical study on dissimilar Friction Stir welding of aluminum 1050 to brass (CuZn30). Materials Science and Engineering: A. 528(22-23):7093-7102.

[2] ASM International Handbook Committee. 1992. Properties and selection: nonferrous alloys and special-purpose materials. ASM International. 2:1143-1144.

[3] Pietrzyk, M., Cser, L. and Lenard, J.G. 1999. Mathematical and physical simulation of the properties of hot rolled products. Elsevier.

[4] Xue, P., Ni, D.R., Wang, D., Xiao, B.L. and Ma, Z.Y. 2011. Effect of friction stir welding parameters on the microstructure and mechanical properties of the dissimilar Al–Cu joints. Materials Science and Engineering: A. 528(13-14):4683-4689.

[5] Zum FÜgen, E., Von Halbzeugen, A., Pour, S. and La Jonction, D. 2005. Friction stir welding—innovative technology for joining aluminium components. Otto Graf Journal. 16:185-97.

[6] Saeid, T., Abdollah-Zadeh, A. and Sazgari, B., 2010. Weldability and mechanical properties of dissimilar aluminum–copper lap joints made by friction stir welding. Journal of Alloys and Compounds. 490(1-2):652-655.

[7] Mahoney, M.W., Rhodes, C.G., Flintoff, J.G., Bingel, W.H. and Spurling, R.A. 1998. Properties of friction-stir-welded 7075 T651 aluminum. Metallurgical and Materials Transactions A. 29(7):1955-1964.

[8] Otegui, J.L. and Fazzini, P.G. 2004. Failure analysis of tube–tubesheet welds in cracked gas heat exchangers. Engineering Failure Analysis. 11(6):903-913.

[9] Liu, H.J., Shen, J.J., Xie, S., Huang, Y.X., Cui, F., Liu, C. and Kuang, L.Y. 2012. Weld appearance and microstructural characteristics of friction stir butt barrier welded joints of aluminium alloy to copper. Science and Technology of Welding and Joining. 17(2):104-110.

[10] Bhamji, I., Moat, R.J., Preuss, M., Threadgill, P.L., Addison, A.C. and Peel, M.J. 2012. Linear friction welding of aluminium to copper. Science and Technology of Welding and Joining. 17(4):314-320.

[11] Esmaeili, A., Rajani, H.Z., Sharbati, M., Givi, M.B. and Shamanian, M. 2011. The role of rotation speed on intermetallic compounds formation and mechanical behavior of friction stir welded brass/aluminum 1050 couple. Intermetallics. 19(11):1711-1719.

[12] Shojaeefard, M.H., Akbari, M., Khalkhali, A., Asadi, P. and Parivar, A.H. 2014. Optimization of microstructural and mechanical properties of friction stir welding using the cellular automaton and Taguchi method. Materials & Design. 64: 660-666.

[13] Beygi, R., Kazeminezhad, M. and Kokabi, A.H. 2012. Butt joining of Al–Cu bilayer sheet through friction stir welding. Transactions of Nonferrous Metals Society of China. 22(12): 2925-2929.

[14] Bisadi, H., Tavakoli, A., Sangsaraki, M.T. and Sangsaraki, K.T. 2013. The influences of rotational and welding speeds on microstructures and mechanical properties of friction stir welded Al5083 and commercially pure copper sheets lap joints. Materials & Design. 43: 80-88.